Inverse Point Kinetics

Introduction

When modeling the behavior of a system, one can often think of the physical system as acting on the independent inputs to produce a particular output response that is related to the input and to the inherent dynamics for the system of interest. This rather abstract view is illustrated for the general case of input u(t) and output y(t) on the left side of Fig. 1, and a specific application of this input-output perspective as applied to the point kinetics equations is given on the right side, where the externally-applied reactivity, ρ(t), is the input and the transient reactor power, P(t), is the output of interest. This is the usual situation that is encountered in modeling most systems and, in particular, when simulating the dynamic behavior of nuclear reactor cores. For example, a routine power maneuver can be simulated by inserting some small positive reactivity [or by moving a control rod or blade outward, which is then converted into an appropriate ρ(t)] and, once the desired power level is achieved, one simply returns the applied reactivity (or control device) back to its original value and allows the system to approach steady state at the new desired power level. The key element in this "usual" for "forward" view is that the reactivity is the driving function or system input and the power level is the output response -- this is the usual input-output view of the system.

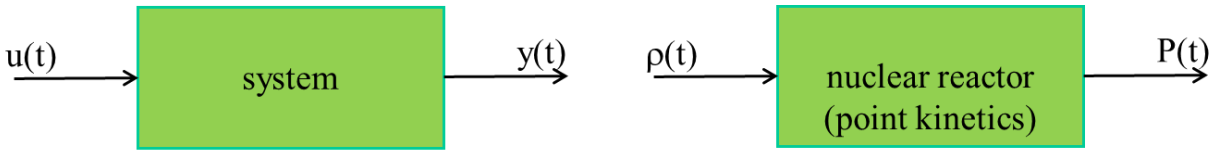

Fig. 1 Usual input-output view of a generic system and a specific reactor dynamics model.

Now, let's reverse our perspective somewhat and ask the question "Given some observed output y(t), what was the input u(t) that caused this output response?". This perspective is referred to as the **inverse problem** -- that is, trying to determine the driving function u(t) that led to some observed system behavior, y(t). And, in the context of reactor dynamics, this is called **inverse kinetics**, where the goal is to determine ρ(t) by observing the P(t) behavior. This "inverse" view of the system is illustrated in Fig. 2 for the reactor dynamics problem, which simply reverses the arrows and the input-output relationships relative to the sketch given in Fig. 1. Thus, in the inverse problem, the signal flow is reversed -- that is, given the observed power vs. time behavior, P(t), as the known "input", we want to compute the "output" ρ(t). This perspective is quite different in that we put on our "detective hat" and by observing some measureable system behavior, we try to determine what actually caused the observed response. This is the goal of all inverse problems...

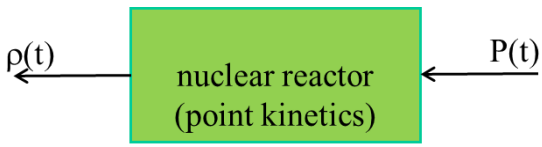

Fig. 2 Input-output view for the inverse reactor dynamics problem.

The Inverse Point Kinetics Equations

Our starting point for the development of **Inverse Point Kinetics** is the **Generation Time Formulation of Point Kinetics**. From Refs. 1 and 2, the Generation Time Formulation of the kinetics equations can be written as

$$\frac{d}{dt}P(t) = \frac{(\rho-\beta)}{\Lambda}P(t) \quad + \quad \sum_i \lambda_i c_i(t) \quad + \quad \frac{\kappa}{\nu}\frac{1}{\Lambda}\langle Q(t)\rangle \tag{1}$$

$$\frac{d}{dt}c_i(t) = \frac{\beta_i}{\Lambda}P(t) \quad - \quad \lambda_i c_i(t) \qquad \text{for } i = 1, 2, \cdots 6 \tag{2}$$

where P(t) is the power level in watts and <Q(t)> represents the total external source strength in neutrons/sec. In the usual forward treatment, time, t, is the independent variable, $\rho(t)$ and <Q(t)> are the system inputs, and the power level, P(t) is the desired output. However, as described above, for inverse kinetics, we reverse the roles of $\rho(t)$ and P(t) -- where now P(t) is known and our goal is to determine the $\rho(t)$ the led to the currently observed P(t) behavior. Thus, the goal here is to solve this set of seven coupled ODEs for the reactivity, $\rho(t)$, given a measured P(t) profile.

To accomplish this goal, we start by solving eqn. (2) for the normalized precursor concentration, then substitute this into eqn. (1), and eventually solve the resultant expression for $\rho(t)$. As a first step, we rearrange eqn. (2) to put it into standard form for solution via the integrating factor method. Doing this gives

$$\frac{d}{dt}c_i(t) + \lambda_i c_i(t) = \frac{\beta_i}{\Lambda}P(t)$$

and multiplication by the integrating factor $e^{\lambda_i t}$ gives

$$e^{\lambda_i t}\left(\frac{d}{dt}c_i(t) + \lambda_i c_i(t)\right) = \frac{d}{dt}\left(e^{\lambda_i t}c_i(t)\right) = \frac{\beta_i}{\Lambda}e^{\lambda_i t}P(t)$$

Now, we multiply both sides by dt and integrate over discrete time interval t_{j-1} to t_j, to give

$$\int_{t_{j-1}}^{t_j} d\left(e^{\lambda_i t}c_i(t)\right) = \frac{\beta_i}{\Lambda}\int_{t_{j-1}}^{t_j} e^{\lambda_i t}P(t)\,dt$$

$$e^{\lambda_i t_j}c_i(t_j) = e^{\lambda_i t_{j-1}}c_i(t_{j-1}) + \frac{\beta_i}{\Lambda}\int_{t_{j-1}}^{t_j} e^{\lambda_i t}P(t)\,dt$$

or $$c_i(t_j) = e^{-\lambda_i \Delta t}c_i(t_{j-1}) + \frac{\beta_i}{\Lambda}e^{-\lambda_i t_j}\int_{t_{j-1}}^{t_j} e^{\lambda_i t}P(t)\,dt \tag{3}$$

where $\Delta t = t_j - t_{j-1}$ is the sampling time used for the measured power vs. time information -- that is, $P(t) \rightarrow P(t_j) = P_j$ is assumed to be available at each discrete time point t_j.

With respect to the integral contained in eqn. (3), we will use the same approach as discussed in Ref. 3. Here T. P. Michaud studied the accuracy of the inverse kinetics method for different integral approximations and came to the conclusion that Simpson's 1/3 Rule[4] gave sufficient

precision with a relatively straightforward implementation scheme. In particular, Simpson's 1/3 Rule applied over an interval $a \le x \le b$ is given by

$$\int_a^b f(x)\,dx \approx \frac{b-a}{6}\left[f(a) + 4f\left(\frac{a+b}{2}\right) + f(b) \right]$$

and using this general result for the integral in eqn. (3) gives

$$\int_{t_{j-1}}^{t_j} e^{\lambda_i t} P(t)\,dt \approx \frac{\Delta t}{6}\left[e^{\lambda_i t_{j-1}} P_{j-1} + 4\left\{ e^{\lambda_i (t_{j-1}+t_j)/2}\left(\frac{P_{j-1}+P_j}{2}\right)\right\} + e^{\lambda_i t_j} P_j \right]$$

Finally, we substitute this expression in eqn. (3) to give

$$c_i(t_j) = e^{-\lambda_i \Delta t} c_i(t_{j-1}) + \frac{\beta_i}{\Lambda} e^{-\lambda_i t_j}\,\frac{\Delta t}{6}\left[e^{\lambda_i t_{j-1}} P_{j-1} + 4\left\{ e^{\lambda_i (t_{j-1}+t_j)/2}\left(\frac{P_{j-1}+P_j}{2}\right)\right\} + e^{\lambda_i t_j} P_j \right]$$

or
$$c_{ij} = e^{-\lambda_i \Delta t} c_{i,j-1} + \frac{\beta_i}{\Lambda}\frac{\Delta t}{6}\left[e^{-\lambda_i \Delta t} P_{j-1} + 2e^{-\lambda_i \Delta t/2}\left(P_{j-1}+P_j\right) + P_j \right] \qquad (4)$$

Thus, eqn. (4) says that, with measured discrete values for the power vs. time, P_j, we can also easily estimate the time-dependent normalized precursor concentrations, c_{ij}, for each precursor group i.

Now, evaluating eqn. (1) at time point t_j using a central finite difference approximation for the derivative, gives

$$\left.\frac{dP}{dt}\right|_{t_j} \approx \frac{P_{j+1}-P_{j-1}}{2\Delta t} = \frac{\left(\rho_j - \beta\right)}{\Lambda} P_j + \sum_i \lambda_i c_{ij} + \frac{\kappa}{\nu}\frac{1}{\Lambda}\left\langle Q_j \right\rangle$$

and, solving this expression for the reactivity at the j^{th} time point, gives

$$\rho_j = \beta + \frac{\Lambda}{P_j}\left[\frac{P_{j+1}-P_{j-1}}{2\Delta t} - \sum_i \lambda_i c_{ij} - \frac{\kappa}{\nu}\frac{1}{\Lambda}\left\langle Q_j \right\rangle \right] \qquad (5)$$

Equation (5) coupled with eqn. (4) for the precursor concentrations, c_{ij}, represent the final form of the desired **Inverse Point Kinetics** equations. With measured values for P_j, these expressions allow us to estimate the reactivity vs. time profile, ρ_j, that actually caused the observed power vs. time behavior to occur.

A Simulated Test of the Inverse Kinetics Method

As a test of the above inverse kinetics methodology, we can solve the "usual" or "forward" point kinetics equations using a standard ODE solver for some specified $\rho(t)$ to determine P(t), and then use the inverse method with this simulated P(t) profile to obtain the "measured" $\rho(t)$ that originally caused the observed P(t) behavior. If this simple test returns the result that $\rho_{measured}(t) \approx \rho_{applied}(t)$, then we will have proven that the theoretical development is sound and that the specific implementation is valid (within the limits of the approximations made during the above development). This approach was successfully applied to test the implementation done in Ref. 3, and here we will use a code that contains only minor modifications to the original code written

by T. P. Michaud. In particular, the **invkin_sr.m** routine which implements eqns. (4) and (5) with no source present, along with the **test_invkin.m** code to evaluate a specific test sequence, will be used here to validate the overall methodology for reference critical operation.

The applied ρ(t) scenario involves a ramped positive insertion, a short interval where ρ(t) is constant, and then a ramped ρ(t) back down to the original zero reactivity level. After a short interval, this sequence is repeated in the reverse order, where the initial change is a negative ramped insertion, and after this second sequence is complete, ρ(t) = 0 is held for an indefinite time. This full ρ(t) sequence is pictured in the top portion on the left side of Fig. 3 and the corresponding simulated normalized power profile is displayed in the lower half of this plot -- where this was generated by solving the forward point kinetics equation with Matlab's built-in **ode15s** ODE solver.

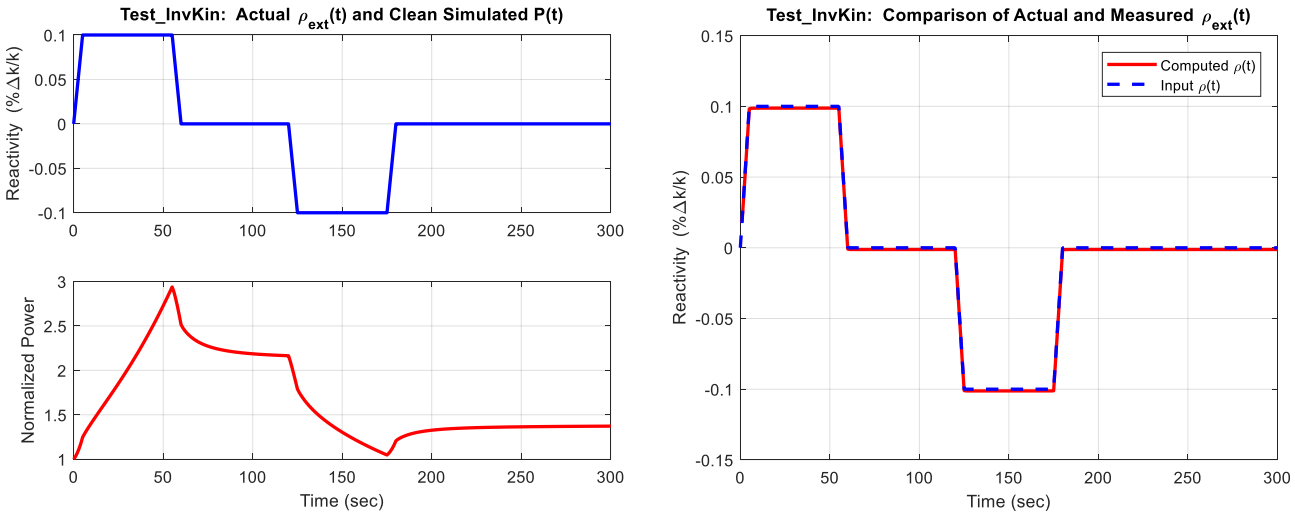

Fig. 3 Results from the test_invkin.m code using the clean simulated P(t).

As apparent, the resultant P(t) profile is as expected, with an increasing power level as the initial response to the positive reactivity at the start of the transient. At about 60 seconds into the transient, a ramped negative reactivity is inserted to counter the original positive reactivity, and we see the power begin to decrease accordingly, eventually approaching a new equilibrium P(t) after about 100 seconds or so into the transient simulation. A similar response is observed as a consequence of the negative-then-positive ramped reactivity perturbations made during the second sequence of reactivity variations in the system. Eventually the system stabilizes at a power level that is about 40% higher than the original P_o.

Now, the real goal of this test sequence was to illustrate and validate the overall inverse kinetics methodology developed in the previous section of these Lecture Notes. To accomplish this, the simulated P(t) profile was used as the input to the **invkin_sr.m** routine, and the computed or "measured" ρ(t) output is compared to the actual input ρ(t) in the right half of Fig. 3 -- and clearly the good comparison here proves the validity of the basic inverse kinetics method and its specific implementation within the **invkin_sr.m** Matlab function file. Several additional test cases showing similar good agreement are also given in Ref. 3.

As a final observation, we should caution that the inverse kinetics method is actually somewhat sensitive to a noisy P(t) signal since it interprets rapid changes in power as being caused by prompt changes in reactivity. To illustrate this behavior, a random ± 5% noise component was added to the simulated P(t) profile from the above test case before sending it to the **invkin_sr.m** routine, and the noisy P(t) input and resultant computed ρ(t) response are shown in Fig. 4. Although this sensitivity to a noisy signal is somewhat problematic, it is clear that the measured ρ(t) output does indeed follow the real applied reactivity that created the P(t) profile. This type of noisy ρ(t) output should be expected in all practical applications of the inverse kinetics method.

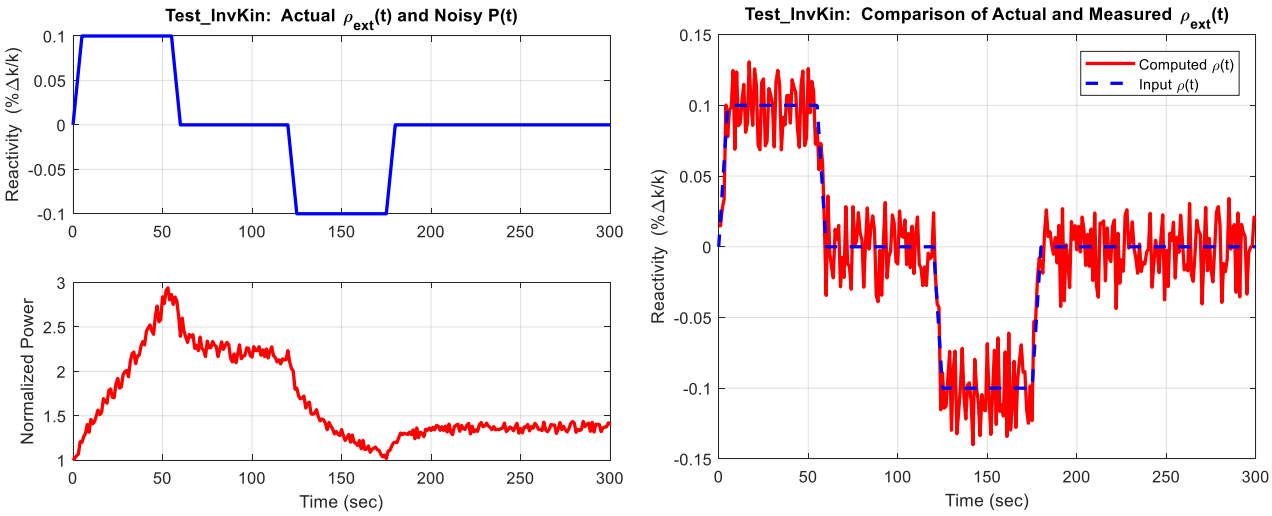

Fig. 4 Results from the test_invkin.m code with a 5% noise component added to P(t).

Implementation Considerations

For implementation of the inverse kinetics equations for use within the UMass-Lowell research reactor (UMLRR), Thomas Michaud, as part of his MS thesis[3], concluded that, for near critical operation, an average of the linear power 1 and 2 channels gave the best P(t) signal to use within eqns. (4) and (5) for evaluating ρ(t). In addition, as part of his work, he also discovered that, at low reactivity levels, there was a "drift" in the reactivity prediction due to gamma interference within the power detectors. In particular, the power data measured by the three power channels (the Linear 1 and 2 channels and the LogPower signal) are not solely related to the neutron signal, but rather they represent a combination of the neutron and the gamma signals. At near critical operation at relatively high power levels (above 500 W), this is not an issue since the neutron signal dominates. However, for fast negative transients, the neutron level drops much faster than the gamma level because of the longer-lived fission product gammas and, during the transient, the assumption that the detector signal is simply proportional to the neutron level may no longer be valid -- and this can lead to significant discrepancies with the inverse kinetics method (i.e. the observed reactivity "drift" noted in Ref. 3). Thus, for practical implementation within the UMLRR for near critical operation, the deviation from critical should be held within about ± 0.4 %Δk/k and the power swing, especially on the low side, should not be much greater that a factor of 10-20 below the reference critical value. Within these rough limits, the inverse

kinetics method proved to be an excellent technique for measuring the dynamic reactivity within the UMLRR (see Ref. 3 for several example test scenarios).

Finally, we note that, although the inverse kinetics method should also be applicable within subcritical configurations, the startup counter within the UMLRR is simply too noisy for practical operation with the current detector system. Thus, our use of the inverse kinetics method within the UMLRR is currently limited to the measurement of dynamic reactivity changes from critical, where the power deviations from reference are such that the power channels are still primarily sensitive to the neutron level (i.e. with minimal gamma interference).

However, even within the limitations noted here, the inverse kinetics method can be extremely useful -- such as for measuring the integral blade worth curves for the various control devices within the system. In particular, an illustration of the procedure for performing a blade calibration using inverse kinetics is incorporated as one of the standard labs within the Reactor Experiments course offered at UMass-Lowell.[5] In addition, it should be noted that the Inverse Kinetics Method has recently replaced the Asymptotic Period Method as the primary means for performing the annual control blade calibrations within the UMLRR[6] -- since the method offers better overall accuracy and a full set of integral worth curves can be generated in only a fraction of the time relative to the traditional Stable Period Method.[7-9] Thus, the **Inverse Point Kinetics** method discussed within these Lecture Notes is indeed a practical tool for measuring reactivity in real reactor operations...

References

1. J. R. White, "One-Speed Point Kinetics Equations," part of a series of Lecture Notes for the Nuclear Engineering Program at UMass-Lowell.
2. J. R. White, "Normalization of the Generation Time Formulation of the One-Speed Point Kinetics Equations," part of a series of Lecture Notes for the Nuclear Engineering Program at UMass-Lowell.
3. T. P. Michaud, "Implementation of the Inverse Kinetics Method for Reactivity Calculations at the UMLRR," M.S. Thesis in Energy Engineering (Nuclear Option), UMass-Lowell, (Dec. 2011).
4. S. C Chapra, **Applied Numerical Methods with Matlab for Engineers and Scientists**, 3rd Ed., McGraw Hill, New York, NY (2012).
5. J. R. White, "Lab Description/Procedure: Measuring Integral Blade Worth Curves within the UMLRR," one of a series of labs for the Reactor Experiments course at UMass-Lowell.
6. Private communications, Leo M. Bobek, Reactor Supervisor, to J. R. White, September 2012.
7. J. R. White, "Blade Worth Calibration Experiment," part of a series of Demos & Expts. available at www.nuclear101.com.
8. J. R. White, "Analysis of Regulating Blade Calibration Experiment #1 Performed on August 3, 2005," part of a series of Demos & Expts. available at www.nuclear101.com.
9. J. R. White, "Analysis of Blade #4 Calibration Experiment #1 Performed on August 15, 2005," part of a series of Demos & Expts. available at www.nuclear101.com.